



Article

Synthesis and Characterization of 2-Decenoic Acid Modified Chitosan for Infection Prevention and Tissue Engineering

Carlos Montez Wells ¹, Emily Carol Coleman ¹, Rabeta Yeasmin ¹, Zoe Lynn Harrison ¹, Mallesh Kurakula ¹, Daniel L. Baker ², Joel David Bumgardner ¹, Tomoko Fujiwara ² and Jessica Amber Jennings ¹,*

- Department of Biomedical Engineering, The University of Memphis, Memphis, TN 38152, USA; cwells3@memphis.edu (C.M.W.); cclman22@memphis.edu (E.C.C.); ryeasmin@memphis.edu (R.Y.); zlhrrson@memphis.edu (Z.L.H.); mkrakula@memphis.edu (M.K.); jbmgrdnr@memphis.edu (J.D.B.)
- Department of Chemistry, The University of Memphis, Memphis, TN 38152, USA; dlbaker@memphis.edu (D.L.B.); tfjiwara@memphis.edu (T.F.)
- * Correspondence: jjnnings@memphis.edu; Tel.: +1-256-310-3153

Abstract: Chitosan nanofiber membranes are recognized as functional antimicrobial materials, as they can effectively provide a barrier that guides tissue growth and supports healing. Methods to stabilize nanofibers in aqueous solutions include acylation with fatty acids. Modification with fatty acids that also have antimicrobial and biofilm-resistant properties may be particularly beneficial in tissue regeneration applications. This study investigated the ability to customize the fatty acid attachment by acyl chlorides to include antimicrobial 2-decenoic acid. Synthesis of 2-decenoyl chloride was followed by acylation of electrospun chitosan membranes in pyridine. Physicochemical properties were characterized through scanning electron microscopy, FTIR, contact angle, and thermogravimetric analysis. The ability of membranes to resist biofilm formation by *S. aureus* and *P. aeruginosa* was evaluated by direct inoculation. Cytocompatibility was evaluated by adding membranes to cultures of NIH3T3 fibroblast cells. Acylation with chlorides stabilized nanofibers in aqueous media without significant swelling of fibers and increased hydrophobicity of the membranes. Acyl-modified membranes reduced both *S. aureus* and *P. aeruginosa* bacterial biofilm formation on membrane while also supporting fibroblast growth. Acylated chitosan membranes may be useful as wound dressings, guided regeneration scaffolds, local drug delivery, or filtration.

Keywords: chitosan; biomaterials; electrospun; acylation; antimicrobial; local delivery



Citation: Wells, C.M.; Coleman, E.C.; Yeasmin, R.; Harrison, Z.L.; Kurakula, M.; Baker, D.L.; Bumgardner, J.D.; Fujiwara, T.; Jennings, J.A. Synthesis and Characterization of 2-Decenoic Acid Modified Chitosan for Infection Prevention and Tissue Engineering. *Mar. Drugs* 2021, 19, 556. https://doi.org/10.3390/md19100556

Academic Editor: Hitoshi Sashiwa

Received: 13 August 2021 Accepted: 27 September 2021 Published: 29 September 2021

Publisher's Note: MDPI stays neutral with regard to jurisdictional claims in published maps and institutional affiliations.



Copyright: © 2021 by the authors. Licensee MDPI, Basel, Switzerland. This article is an open access article distributed under the terms and conditions of the Creative Commons Attribution (CC BY) license (https://creativecommons.org/licenses/by/4.0/).

1. Introduction

Chitosan is considered a promising therapeutic delivery agent due to its biodegradability, biocompatibility, non-toxicity, and inherent antimicrobial activity [1,2]. Chitosan is a sugar-based biopolymer derived from exoskeletons of arthropods, e.g., crustaceans and insects, fungi cell walls, mollusks radulae, fish scales, cephalopod beaks, and lissamphibian skin. Structurally, chitosan is a heteropolymer composed of N-acetyl-D-glucosamine and D-glucosamine unit connected through β (1-4) glycosidic bond. Chitosan has three reactive functional groups: an amine group at the C-2 position, and primary and secondary hydroxyl groups at C-6 and C-3 positions, respectively. Chitosan is polycationic at a pH below six and interacts with negatively charged molecules, such as proteins, anionic polysaccharides, fatty acids, bile acids, and phospholipids [3]. Chitosan is a versatile polymer due to its flexibility that allows manufacturing into various forms such as gels, nanofibers, pastes, films, etc. Electrospun chitosan membranes are of particular interest for biomedical applications due to their porous nanofibers and high surface area that mimics the extracellular matrix. Multiple biomedical applications, including wound dressings, drug delivery, and tissue engineering, involve nanofibrous chitosan membranes [4,5].

Chemical modification of electrospun chitosan membranes can enhance their physicochemical properties, further functionalizing the material to allow for a broader range of Mar. Drugs 2021, 19, 556 2 of 13

applications. For example, the incorporation of hydrophobic substituents, such as fatty acids, generates a domain for absorbing and carrying poorly soluble drugs. Literature supports the potential for fatty acid (FA)-treated chitosan membranes to control the release of the hydrophobic drug simvastatin [6]. Linoleic and α -linolenic acid-modified chitosan has demonstrated potential as a multifunctional catheter coating by improving the lubricity and antimicrobial properties [7]. A study also found that fatty acid incorporated chitosan can improve mucoadhesive properties in a self-nano-emulsifying drug delivery system [8]. Studies investigated decanoic acid grafted chitosan as a potential carrier of insulin by combining the mucoadhesive and permeative properties of chitosan and decanoic acid, respectively [9]. Decanoic, oleic, and linoleic acid-modified chitosan have enhanced wound healing rates [10,11]. The length of the fatty acyl chain incorporated through O-acylation can control the chitosan nanofiber's crystal structure. It also improves its stability in the moist environment while maintaining its non-toxic property and has shown promise for regenerating bone in guided bone regeneration (GBR) applications in rodent models [12–14]. A study using buriti oil containing volatile compounds and fatty acids indicated that chitosan and buriti oil could be combined into a gel to improve chemical properties and activity against Gram-negative pathogens [15]. In addition to the antimicrobial activity, chitosan gel with buriti showed antioxidant and anti-inflammatory properties, good healing activity, and an adequate wound retraction rate [15].

Trifluoroacetic acid (TFA) is one of the most commonly used solvents for electrospinning chitosan membranes because it provides adequate viscosity for the polymer solution to be pulled into nanofibers [6,16]. Despite this benefit, TFA forms a salt with chitosan's amino groups, requiring removal without compromising the nanofibrous structure or deteriorating the membrane's mechanical properties. One technique to achieve this balance involves grafting fatty acid (FA) groups to the hydroxyl groups outside of the chitosan fibers to create a hydrophobic covering to prevent fiber swelling during the washing steps of TFA ions [13]. FA chains can be attached to any of the three reactive groups; acid chlorides and methanol crosslinks FAs in the amine position [17,18]. Acylation reactions may also use a coupling agent, such as 1-ethyl-3-(3-dimethyl-aminopropyl)-1-carbodiimide hydrochloride (EDC) to improve the reactivity [7]. The TFA salt in the electrospun chitosan membrane occupies the amine group [16]. Wu et al. developed an O-acylation method in which the chitosan membrane is acylated by acid anhydride in the presence of a pyridine catalyst to improve its stability in an aqueous solution [12,14].

The fatty acid 2-decenoic acid (2DA) and its analogs are medium chain FA chemical messengers naturally produced by bacteria. Studies have shown that the *cis* form of 2DA (C2DA) disperses existing biofilm and inhibits biofilm formation [19]. Studies suggest that 2DA could increase microbes' metabolic activity and the bactericidal ability of commonly used antimicrobials [20]. These properties could make 2DA a potential complementary therapy for infection. Additionally, 2DA could lessen antibiotic tolerance by improving the efficacy of these drugs against biofilm infection. Acylating chitosan membranes with 2DA or analogs may provide the advantages of bacterial biofilm resistive materials and the ability to load with hydrophobic therapeutics for extended release. However, 2-decenoyl chloride (2DC) is not commercially available. This study investigates a custom synthesis route for acyl chlorides and their ability to stabilize and functionalize chitosan nanofibers. Additionally, this study determined physicochemical properties, antimicrobial properties, and cytocompatibility of acyl-modified chitosan nanofibers [21].

2. Results

2.1. Viscosity Average Molecular Weight

The intrinsic viscosity (η) of the chitosan used for electrospinning membranes was determined to be 6.249. The calculated viscosity average MW was 664.7 kDa.

Scanning electron microscope images showed that fibers formed and stabilized by each acylation method without significant swelling (Figure 1). No significant differences in fiber diameter were detected between treated groups and as-spun membranes (Figure 2).2. Fibrating electron microscope images showed that fibers formed and stabilized by

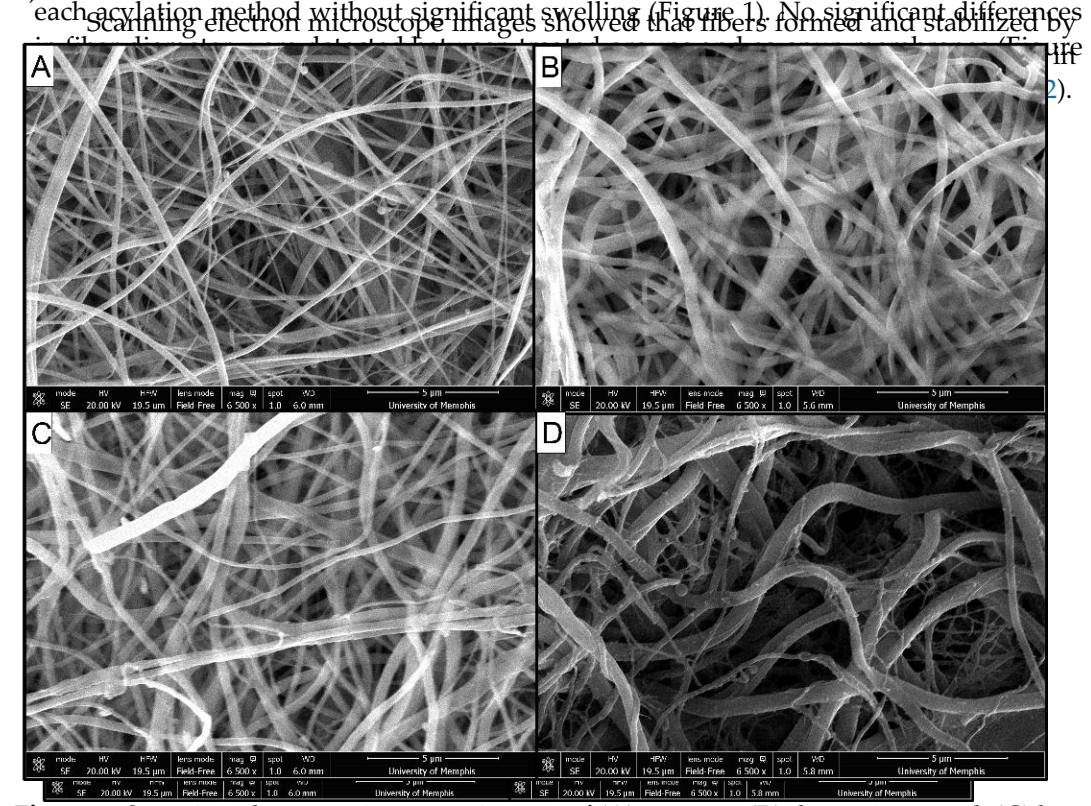


Figure 1. Scanning electron microscope images of (A) as-spun, (B) decanoic treated, (C) hexanoic treated and (D) 2-december in ages of (A) as-spun, (B) decanoic treated, (C) hexanoic treated and (D) 2-december in ages of (A) as-spun, (B) decanoic treated (C) hexanoic treated, and (D) 2-december treated membranes at 6500 × magnification.

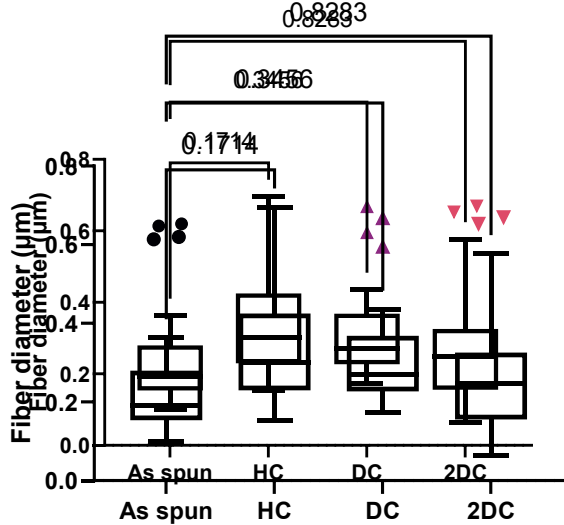


Figure 2. Boxplot shows fiber diameters after acylation. Numbers above connected lines are *p*-**Figure 2.** Boxplot shows fiber diameters after acylation. Numbers above connected lines are *p*-values **Figure 2.** Boxplot shows fiber diameters after acylation. Numbers above connected lines are *p*-tor comparisons. Outliers are shown as individual points. values, for comparisons. Outliers are shown as individual points.

2.3. Fourier Transform Infrared (FTIR)

2.3. Fourier Transform Infrared (FTIR)

2.3. Fourier Transform Infrared (FTIR)

2.3. Follage Health of the Source of the Sourc

Mar. Drugs 2021, 19, x FOR PEER REVIEW 4 of 13

Mar. Drugs 2021, 19, 556

membranes represent NH2. The lack of peaks < 1000 cm⁻¹ in treated membranes confirm

the removal of TFA salts [142] the lack of peaks < 1000 cm⁻¹ in treated membranes confirms

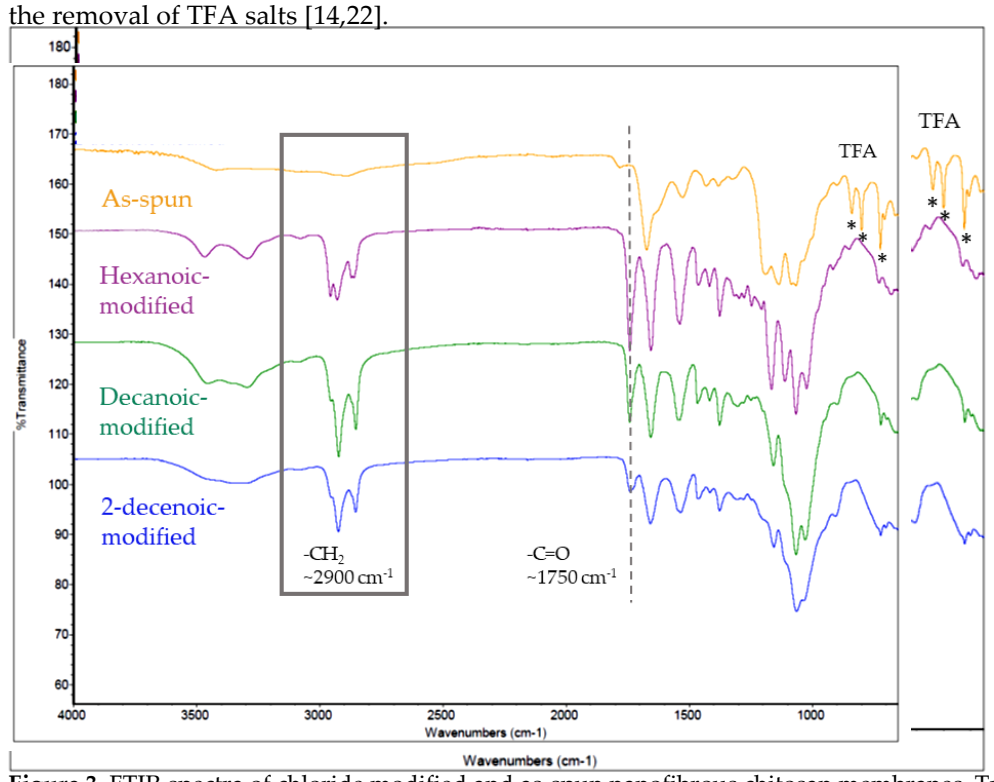
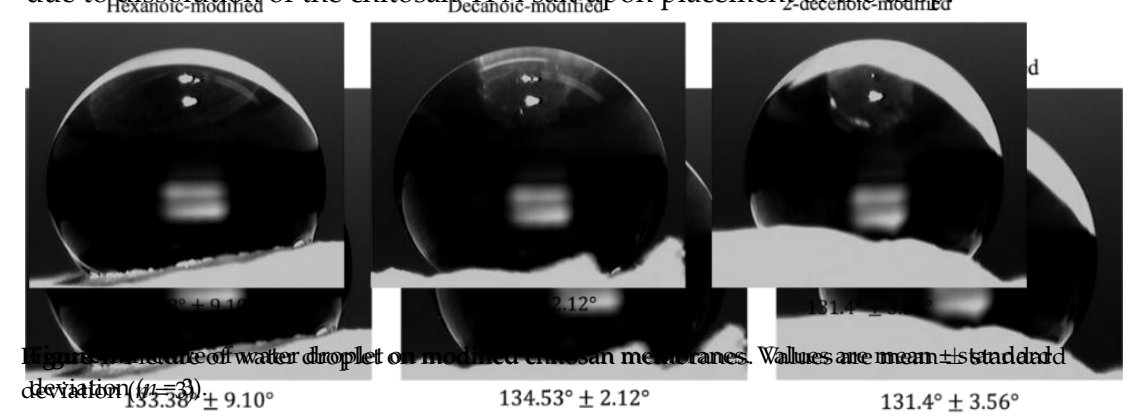


Figure 3. FTIR spectra of chloride modified and as-spun nanofibrous chitosan membranes. Trans-**Higure 3. FTIR spectra of chloride modified in the characteristic manufacture of the characteristic the cha**

2.4. Contact Angle

2.4. (Water throughts remained stable on modified membranes for more than 5 min (Figure 4). Awater droplets remained stable on modified membranes for more than 5 min (Figure 4). Away of all the treatments decay to the droplets of the membranes were the most min (Figure 4). Among all the treatments decay to the droplets of the childs of the childs of the droplets o



Proute Medical Medical Medical Medical Medical Medical Chitosan membranes. Values are mean ± standard deviational Different Medical Me

decanoic-, and 2-decenoic- modified membranes, respectively (Table 1).

100

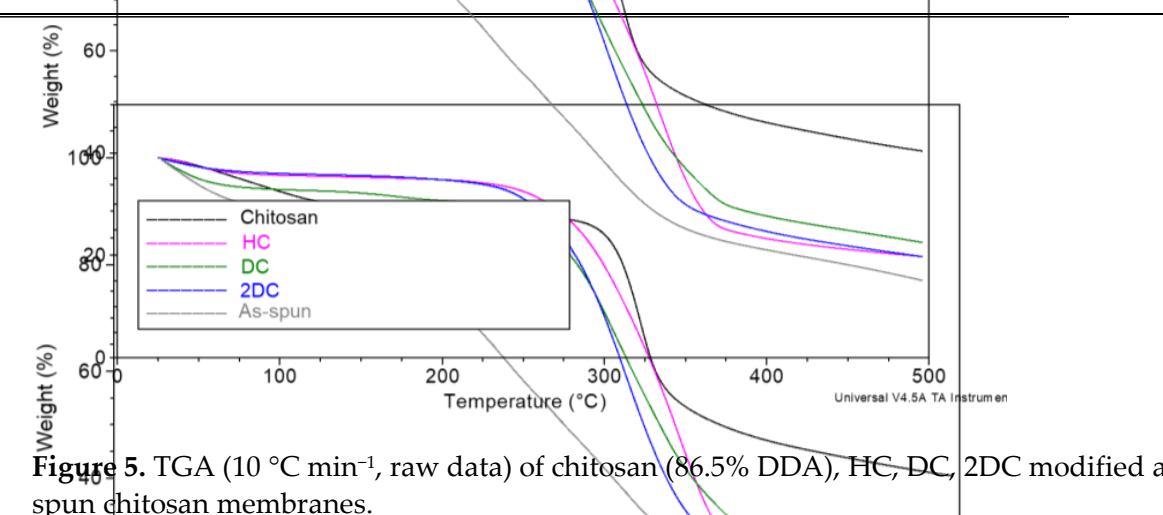


Table 1. Summary of TGA analysis for HC, DC, and 2DC modified chitosan membranes, and chitosan (86.5% DDA

			1				
		Weight Loss (%	(a) As	s-spun Weight lo	ss w/o water (%)	T _D (I) (°C)	To (on
Sample	Water	Deg-1 ₀	Remaining	Deg-1 (norm)	Remaining (norn	n) Dog 1 in Hatian	Dec 1
	rt-150 °C	150–500 °C	⁰ at 500 °C	100 150–500°€ ⁰⁰	at 500 °C	400 Deg-1 initiation	Deg-1
Chitosan	11	49	40	55	45	263	2
HC	4	76 Figure 5	5. TOA (10	nin ⁻¹ , raw data) of chit C min ⁻¹ , raw da	tosan (86,5% DDA), HC. ta) of chitosan (86.5	DC-2DC modified and as-spun % DDA), HE, DC, 2DC	modifi 2
DC	8	69 spun (i membranès. Chitosan me	mbranes?5	25	217	2
2DC	Table 13 Sumn	nary of ಢ A analys	sis for <u>Þ</u>(C , DC,	and 2DC 1 719 dified ch	itosan memb ra pes, and	chitosan (86.5%)PD A).	2

Table 1. Summarweight Cosanalysis for HC, Dwigned 2D Convalified chitosan membranes, and constassan (86.5% D

	TA7 4		6 hitnean is	2000000000	and one	2 04111000	mmino 1	1911 (('c	Land ()- \ Turith a mo	وليتعمد
Sample	vvalei	Weight Loss	(0/) \\\\\\\\\\\\\\\\\\\\\\\\\\\\\\\\\\\\	ATEONTO SO	Weight	loss w/g	water	11 Initiation	on Tegil Caset	T _P
Sample	Water	Deg-1	Remaining	Deg-1	(norm	a rate al la	naining	(FORM) 6	1 (1) E 2051: (1)	1. 1110
I CHHO <u>San</u>		150–500 °C	a auring the racermonom	s process ver M 15 0-	-500°C	% deace 21 25	at 500°	TISUIC O	, l eft)_g F q aatian (1)	reppe
Chitosa2DC	11 ³	49	20 40	•	55	21	45	212	2663	
HC	4	76	20Aver	age chite	y ssan M	W (86.5°	% DDA)	$= 179 \times ($).865 + 221 5× 0.135 : n a molecylar weight	= 184.7
DC	8								i a molecular weight 50522102117 505221021117 weight	
2DC	3								ion (1) represents the	3 not a
		avera	nomer backt age monomer M	W.	iitosan	. 11115 at	nows un	e trieoren	car carculation for	uegre

stitution (DS) per chitosan unit, which is structurally represented in Figure 6 (ceright). (MW) of 179 and a N-acetyl glucosamine unit (C8H15NO6) with a MW of 221. Tused during this process is 86.5% deacetylated (Figure 6, left). Equation (1) repayerage monomer MW.

HO NH HO Average chitosan MW (86.5% DDA) = 179 × 0.865 + 221 × 0.135 = 18

monomer backbone of chitosan. This allows the theoretical calculation for destitution (DS) per chitosan unit, which is structurally represented in Figure 6 stitution (DS) per chitosan unit, which is structurally represented in Figure 6. Representation of 86.5% deacetylated chitosan units before surface modification with the various chitosan units before surface modification with the various chitosan units before surface modification with the various modified chitosan with a degree of substitution (DS) = 1, and right (DS)

The surface modification of chitosan with the various modifiers does not affect the monomer backbone of chitosan. This allows the theoretical calculation for degree of substitution (DS) per chitosan unit which is structurally represented in 15% allows the theoretical calculation for degree of substitution (DS) per chitosan unit which is structurally represented in 15% allows the following results from Equation (1) and the following calculations, the average of in a write MW and had a tarming of

ing unit MW can be determined. DS=1

Mar. Drugs **2021**, 19, 556 6 of 13

Since fatty acids evaporate with cleavage of the ester linkage at the stage of Deg-1, is can be assumed that the same amount (weight) remains at 500 °C in the original chitosar from Table 1, at 500 °C chitosan has degraded by 55%, which resulted in 45% reand modified chitosan membranes from Equilon in goal culture satisfies the Equilon in goal culture satisfies the Equilon in goal culture satisfies the Equilon in the stage of Deg-1, is an another than the stage of Deg-1, is an action of the stage of Deg-1, is an action of Deg-1

Since fatty (4i84e7ap0888) with C24vag886 The rester 2i1kage at the stage of Deg-1, it can be assumed that the same amount (weight) remains at 500 °C in the original chitosan and modified chitosan membranes. The following calculations estimate the DS per chitosan unit for each suf 184 podif 1841 (C0H25) +88a MW of 180DC ($C_{10}H_{19}O$) has a MW of 154, and 2DC ($C_{10}H_{17}O$) had a MW of 152. Equation (4) estimates DS for HC, Equation (5) estimates DS for DC, and Equation (6) estimates DS for 2DC.

$$(184.7 + 152x) \times 0.21 = 83.1, x = 1.4$$

$$(184.7 + 152x) \times 0.21 = 83.1, x = 2.1$$
(4)

$$(184.7 + 154x) \times 0.25 = 83.1, x = 1.0 \tag{5}$$

2.6. Antimicrobial Activity

 $(184.7 + 152x) \times 0.21 = 83.1, x = 1.4$ (6)

The sponge control had spriftly more CFUs counted than all other groups (Figure 7). The CFU count for sponge control had significantly more CFUs counted than all other groups (Figure 7). The CFU count for hexanoic treated membranes was comparable to the CFU count for hexanoic treated membranes was comparable to the CFU count for the gauze control than and considered membranes was comparable to the CFU count for the gauze control than and considered membranes was comparable to the CFU count for the gauze control treated membranes was significantly less than the gauze control to gauze control.

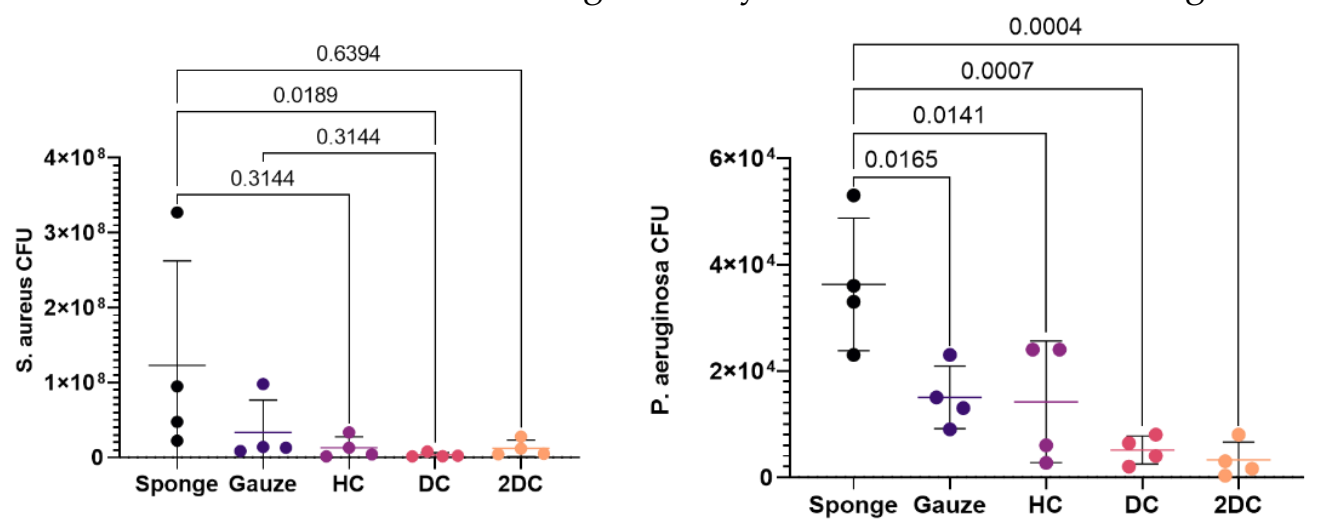
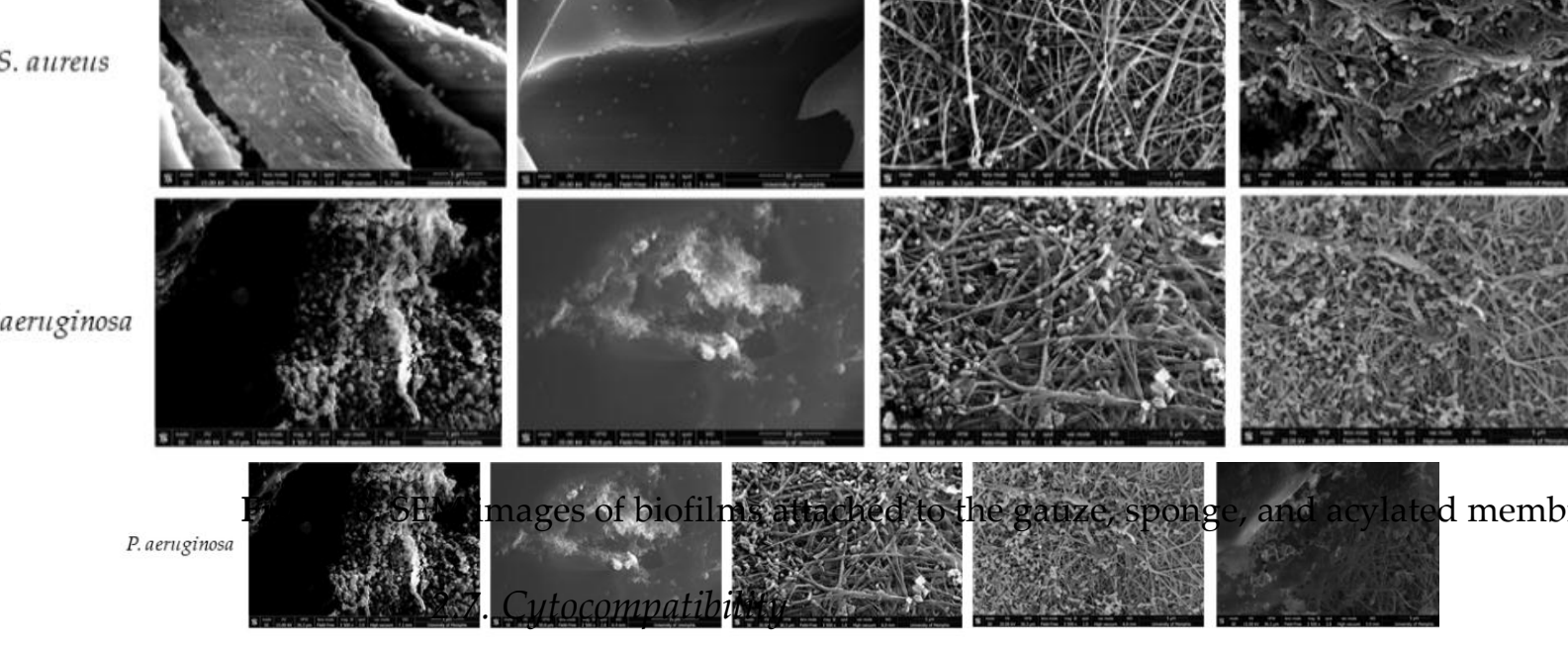


Figure 7. Scatterplot shows colony forming units (individual points shown with lines representing mean ± standard deviation) of S. aureus (left) and P. aeruginosa (right) for the treated membranes were compared with sponge and gauze formed in Scatterplot shows colony forming units (individual points shown with lines representing controls. Numbers above connected lines are p-values between groups.

mean ± standard deviation) of S. aureus (left) and P. aeruginosa (right) for the treated membranes seminanes of biofilm attached to membranes confirmed that some sparse colonies of were compared with spange and gauze controls above remembranes are p-values between groups.

2-decenoic membranes. P. aeruginosa formed abundant EPS on gauze fibers (Figure 8). In contrast, while P. aeruginosa subsisted on acylated membranes, EPS formation was minimal.

SEM images of biofilm attached to membranes confirmed that some sparse colonie of *S. aureus* exist on hexanoic- and decanoic-acylated membranes, with very few observed on 2-decenoic membranes. *P. aeruginosa* formed abundant EPS on gauze fibers (Figure 8) In contrast, while *P. aeruginosa* subsisted on acylated membranes, EPS formation was minimal.



differences and all were above the 70% cytotoxicity threshold, in a 10998-5-Biologicity Exploration of the chiral production of the condition of the condition

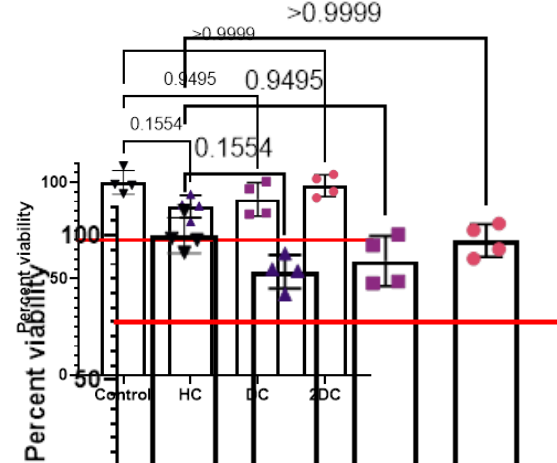


Figure 9. Graph shows cytocompatibility testing of acyl modified membranes in transwell in contact with SIH BT3 cells n = 4). Individual data points are shown as symbols with bars representing mean and error bars representing standard deviation. Red line indicates the 70% cytocompatibility minimum as established by ISO 10993-5.

Figure 9. Graph shows cytocompatibility testing of acyl modified membranes in transwell in contact $\frac{3}{4}$ with $\frac{3}{4}$ cells (n = 4). Individual data points are shown as symbols with bars representing

Figure 9. Crapter shows to the total politics to the first to the modification and additional provides and the compounds accessing the customizable, making previously commercially unavariable compounds accessing in a customizable, making previously commercially unavariable compounds accessing in a customizable, making previously commercially unavariable compounds accessing in a customizable, making previously commercially unavariable compounds accessing in a customizable and respective professional previously commercially unavariable accessional professional professional

Mar. Drugs **2021**, 19, 556 8 of 13

FTIR results indicate immobilization of FAs on the fibers. The absorption peak around $1750~\rm cm^{-1}$ representing the acyl group (C = O) and ester bond formation confirms acylation. Ester bonds may be particularly advantageous for these materials in infection prevention. In the presence of acidic environments, such as those found locally at tissue injury sites or in the presence of bacterial enzymes, such as lipase, they may hydrolyze [19,20]. Environment-influenced hydrolysis may cause acylated chitosan biomaterials to be less reactive until interaction with bacteria or damaged tissue. This study did not measure the hydrolysis rate of fatty acids; future studies will investigate whether conjugated 2DA release is lipase or pH-sensitive. FTIR spectra broad peaks at 3100–3500 cm $^{-1}$ represent inter- and intra-molecular hydrogen bonding of the -NH2 and -OH vibration stretching of chitosan molecules [13]. Of note, TFA-salt representative transmittance peaks at 720, 802, and 837 cm $^{-1}$ are not present in any of the modified chitosan biomaterials that confirm the salts are no longer present.

Water contact angle measurements also validate the acylation process that imparts hydrophobic properties to the hydrophilic chitosan biomaterial. The contact angle results for this study using acyl chlorides are consistent with prior studies that used acyl anhydrides [6,12] in that the contact angle increases with the chain length. Although contact angle on as-spun membranes was not measured, contact angles for acylated membranes are higher than those observed for neutralized chitosan films and coatings (80–100°) in other studies [26,27]. Decanoic acid and 2-decenoic acid have the same chain length, with 2DA having one unsaturated bond. The unsaturated fatty acid should have less hydrophobicity than the saturated decanoic acid, which is consistent with the lower contact angle for 2DA-modified membranes. The variability in contact angle observed in this evaluation may be due to varying degrees of substitution, as well as the rough texture of the nanofibers. A further limitation is that membrane surfaces were not completely flat, which could introduce error or variability to the measurements.

Chitosan is known to thermally degrade in two phases under nitrogen atmosphere; one phase occurs around 300 °C with complete mass loss over 600 °C [28]. As acyl chains cap the hydroxyl groups, membranes become more hydrophobic with less water associated, which explains why less mass of water is lost during the initial phase of TGA for acylmodified membranes. The earlier initiation and onset temperatures for acyl-modified membranes are consistent with other studies of ester-modified chitosans [29,30], and provide additional confirmation that ester linkages are occurring. The larger percentage of total mass lost after the onset of degradation for acyl-modified membranes are likely due to the degradation of alkyl chains, also confirming that acylation was successful. The calculated theoretical degree of substitution for hexanoic-modified membranes is in agreement with values for similar materials obtained by elemental analysis [12]. The DS of 2 for hexanoic-modified membranes suggests that, per chitosan unit, both primary alcohol and secondary alcohol reacted with the hexanoic chloride. The lower degree of substitution for decanoic- and 2-decenoic modified may be due to steric hindrance of the additional carbons on the chains. The higher degree of substitution for 2-decenoic-modified membranes compared with decanoic-modified may be due to the trans-unsaturation point making the carbonyl more accessible for higher reactivity.

Acylated chitosan membranes demonstrated the ability to inhibit bacterial growth and attachment (CFUs). In all antimicrobial testing conditions, the acylating nanofibers showed evidence of reduced biofilm attachment. Surface attachment is a mechanism biofilm uses to develop and persist. Modified chitosan-nanofibrous membranes have more surface area for bacteria to attach than chitosan sponge or gauze and still produced better bacteria inhibition results. These findings support the hypothesis that acyl-modification contributes to improved antimicrobial properties. Acyl-modified materials seem to inhibit *P. aeruginosa* EPS production. Reduction of EPS secretion from *P. aeruginosa* blocks a primary mechanism *P. aeruginosa* uses to form a biofilm, and modified materials may interfere with type IV pili [31–33]. *S. aureus* biofilm inhibitory effects may be due to interference with microbial surface components recognizing adhesive matrix molecules (MSCRAMM). MSCRAMMs are instrumental in *S. aureus* attachment and subsequent biofilm formation [34]. The

Mar. Drugs **2021**, 19, 556 9 of 13

differences in bacterial hydrophobicity/hydrophilicity may explain the differing degrees of response between *S. aureus* and *P. aeruginosa* [35,36]. The high variability observed for CFU counts may be overcome in future studies by using different types of viability assays, such as luciferase-based luminescence assays. When unattached bacteria remain in the planktonic state longer, they are more susceptible to antimicrobials and the innate immune system. In this study *S. aureus* and *P.* aeruginosa were chosen as representative Gram-positive and Gram-negative strains that are common pathogenic strains in bone and wound injuries. More studies of efficacy of modified membranes against other bacterial and fungal strains are necessary to understand their broad antimicrobial efficacy.

Balancing bacterial inhibition with cyto- and bio-compatibility is challenging for many potential antimicrobial biomaterials, drug delivery systems, and tissue regeneration templates [37–40]. All acyl-modified materials demonstrated cytocompatibility with no detectable differences between any of the evaluated groups. All modified membranes met or exceeded the minimum 70% cellular compatibility threshold recommended by the ISO 10993-5 Biological Evaluations of Medical Devices standard [23]. Future studies will evaluate the effects of these materials on other cell types, such as immune cells, and will assess biocompatibility in vivo. While this study did not assess as-spun material as controls due to the rapid dissolution and acidity of these materials, the acyl-modified materials performed similarly to previously investigated chitosan-based materials [6,41–43]. There are no signs of acyl-modified materials adversely affecting cells or any signals that healing would be negatively affected [10].

In summary, modified chitosan biomaterials possess characteristics that support their use in infection prevention treatment strategies. These methods allow for functionalization of chitosan with specific fatty acids. Future studies will evaluate conjugated fatty acid hydrolysis rate in physiological relevant solutions, including acidic and in the presence of enzymes such as lipase. Additional future and ongoing studies will characterize the drug delivery capabilities of acylated nanofiber biomaterials loaded with therapeutics such as local anesthetics, statins, chemotherapeutics, or antimicrobials.

4. Materials and Methods

4.1. Characterization of Viscosity Average Molecular Weight

The average molecular weight of chitosan (Chitolytic; Toronto, ON, Canada) was validated using viscosity measurement. To determine the intrinsic viscosity (η), chitosan was dissolved in various concentrations (0.07, 0.08, 0.13, 0.20 g/dL) 0.25 M acetic acid and 0.25 M sodium acetate and filtered through a 0.45 μ m filter. Flow time of the solvent and different concentrations of CS samples were measured at 25 \pm 0.1 °C using an Ubbelohde viscometer [44]. The intrinsic viscosity and average molecular weight of CS were calculated using the following Mark–Houwink–Sakurada (MHS) equations.

Intrinsic viscosity
$$[\eta] = KM^a$$
 (7)

Viscosity average molecular weight
$$M = ([\eta]/K)^{1/a}$$
 (8)

where viscometric constant $K = 1.57 \times 10^{-3}$ cm³/g and a = 0.79 [45,46] for a solvent of 0.25 M acetic acid and 0.25 M sodium acetate.

4.2. Fabrication of Electrospun Membranes

Nanofibrous chitosan membranes were electrospun using chitosan (86.5% DDA) following previous methods [43]. Briefly, Chitosan was dissolved overnight at 5.5% (w/v) in 70:30% (v/v) TFA and dichloromethane (DCM) purchased from Sigma Fisher (Burlington, MA, USA). The solution was centrifuged to remove any insoluble chitosan, transferred to a syringe with a 20-gauge blunt needle, and electrospun at a rate of 15 μ L min⁻¹ and a voltage of 27 kV using a syringe pump onto an aluminum foil covered collector plate rotating at ~8.4 revolutions per minute, with constant monitoring of the Taylor Cone to ensure high-quality membranes. The electrospinning apparatus was housed inside a

Mar. Drugs **2021**, 19, 556

ventilated box which was vented to a fume hood. The apparatus was operated at room temperature and at 40–60% humidity. Membranes were spun from three 10 mL volumes to obtain a diameter of 15 cm and thickness of approximately 700 μ m. After membranes were fabricated, they were sectioned into 10 mm diameter discs for use in experiments.

4.3. Synthesis of 2-Decenoyl Chloride

A reflux reaction was used to synthesize 2-decenoyl chloride based on the method described by Namazi et al. [47], by first placing 1 M (40 g L $^{-1}$) of sodium hydroxide (NaOH) in a covered beaker on ice. The NaOH beaker was connected to a condenser unit in a water bath set at 35 $^{\circ}$ C. First, thionyl chloride (150 mmol) was added to a three neck round bottom flask. Second, while slightly shaking the flask, 2-decenoic acid (100 mmol) was added. Once both compounds were in the flask, the flask was connected to a condenser system, sealed, and reacted for five hours. After reaction completion, the synthesized 2-decenoyl chloride was removed from the flask and stored until later use. Decanoyl chloride (DC) and hexanoyl chloride (HC) were purchased from Sigma Fisher (USA).

4.4. Acylation Reactions

The direct acylation of chitosan materials by acyl chlorides was achieved by first making a 5 mg mL $^{-1}$ solution of chitosan material in pyridine. With a ratio of 3:1 (v/v) pyridine to acyl chloride, the acyl chloride was slowly added while stirring. The solution reacted for 1.5 h. Once the reaction was complete, the chitosan materials were removed and placed in 10% acetone solution (1 L), then removed and placed in 70% ethanol solution, removed and finally placed in deionized water (DI). Each step lasted for at least one hour. After the final washing step, the chitosan materials were removed from the solution, placed flat onto a glass surface, and frozen at $-80\,^{\circ}$ C. The frozen materials were lyophilized. After lyophilization, the materials were stored in a desiccator until further analysis.

4.5. Scanning Electron Microscopy

Images were acquired using SEM (Nova NANOSEM 650 FEITM, Hillsboro, OR, USA) to determine the effects of acylation on fiber size and surface morphology. Twenty fibers were randomly selected in each image of as-spun and treated membranes and fiber diameter was measured using ImageJ.

4.6. FTIR

Attenuated total reflectance (ATR) Fourier transform infrared (FTIR) spectra were collected with a diamond crystal using an FTIR spectrometer (Frontier, Perkin-Elmer, Waltham, MA, USA). ATR spectra were collected to confirm the attachment of FA groups to the chitosan polymer chain and TFA salt removal by the treatments.

4.7. Thermogravimetric Analysis

Thermogravimetry analysis (TGA) was performed with a TGA-Q50 (TA Instruments, New Castle, DE, USA) under a nitrogen atmosphere. The heating rate was 10 °C/min.

4.8. Contact Angle

Water contact angles of modified membranes were determined using a VCA optima measurement machine (AST products, INC, Billerica, MA, USA) [14]. Water droplets (5 μ L) were placed carefully onto the membrane surfaces. A digital camera recorded the photographs of the droplets after approximately one minute. The goniometry software of VCA OptimaXE calculated the contact angles. For each modification, four different membranes were tested at three regions.

4.9. Antimicrobial Activity

Pseudomonas aeruginosa (P. aeruginosa, ATCC #27317) and Staphylococcus aureus (S aureus, UAMS-1, a clinical osteomyelitis strain) grown overnight were diluted to 1:50 and 1:10,

Mar. Drugs **2021**, 19, 556 11 of 13

respectively. Diluted bacteria (500 μ L) were added to the well containing HC, DC, 2DC modified membranes, sponge, or gauze, and incubated for 24 h. The membranes, sponges, and gauzes were taken out of the solution after the incubation period and washed three times with 500 μ L of 1× phosphate-buffered saline (PBS). They were then immersed in 500 μ L of sterilized tryptic soy broth (TSB) and sonicated for 5 min to detach the bacteria. After sonication, the detached bacteria solution was used for colony forming unit (CFU) counting by plating dilutions.

4.10. Cytocompatibility

NIH 3T3 (American Type Culture Collection, RRID:CVCL_0594) fibroblasts were seeded at a concentration of 10^4 cells cm $^{-2}$ in a 24-well plate in Dulbecco's Modified Eagle's Medium (DMEM) high glucose supplemented with 10% fetal bovine serum (FBS, Gibco) and 2% (100 μ g mL $^{-1}$) Normocin (InvivoGen, San Diego, CA, USA). Chitosan membranes were placed into well inserts and then immersed into the wells containing cells and media. Control wells did not have any materials added (tissue culture plastic). Plates were incubated at 37 °C with 5% carbon dioxide (CO₂). Every 24 h, the inserts were removed, the wells were bright field imaged, and the media was refreshed. After 48 h, viability was determined using CellTiter-Glo® (Promega, Madison, WI, USA) and expressed as a percentage of tissue culture plastic controls.

4.11. Statistical Analysis

SigmaPlot and GraphPad Prism 7.2 software (GraphPad Software Incorporation, La Jolla, CA, USA) was used to perform the statistical analysis. Data were assessed first by performing Shapiro–Wilk normality test, followed by Brown–Forsythe equal variance test. If both passed, a one-way analysis of variance (ANOVA) further analyzed the data, followed by Holm–Sidak post hoc analysis to detect significance between experimental groups ($\alpha = 0.05$). Kruskal–Wallis ANOVA on ranks, followed by Tukey post hoc test, completed additional analysis if necessary normality and equal variance requirements did not occur.

Author Contributions: Conceptualization and methodology, J.A.J., D.L.B. and C.M.W.; validation, formal analysis, investigation, resources, and data curation, C.M.W., E.C.C., R.Y., Z.L.H.; writing—original draft preparation, J.A.J., C.M.W., E.C.C., R.Y., Z.L.H. and M.K.; writing—review and editing, J.A.J., D.L.B., T.F., J.D.B., M.K. and C.M.W.; supervision, project administration, and funding acquisition, J.A.J., C.M.W., J.D.B., D.L.B., T.F. All authors have read and agreed to the published version of the manuscript.

Funding: This research was funded by the National Science Foundation: 1945094 and the FedEx Institute of Technology Development Award.

Institutional Review Board Statement: Not applicable.

Informed Consent Statement: Not applicable.

Data Availability Statement: The data presented in this study are available on request from the corresponding author.

Acknowledgments: We would like to thank Warren O. Haggard for assistance and guidance. Thanks are also extended to Vishnu Priya Murali for assistance with biomaterial fabrication and the initial acylation process. We would like to thank Ezzuddin Abuhussein, Brittany Spencer, Lydia Ross, Alexis Johnson, Landon Choi, and Andrew Blass Watson for assistance with experiments and fabricating biomaterials as well as Omar Skalli, and Lauren Thompson for assistance with SEM imaging.

Conflicts of Interest: The authors declare no conflict of interest.

References

- 1. Goy, R.C.; de Britto, D.; Assis, O.B.G. A review of the antimicrobial activity of chitosan. *Polímeros* 2009, 19, 241–247. [CrossRef]
- 2. Mohebbi, S.; Nezhad, M.N.; Zarintaj, P.; Jafari, S.H.; Gholizadeh, S.S.; Saeb, M.R.; Mozafari, M. Chitosan in Biomedical Engineering: A Critical Review. *Curr. Stem Cell Res. Ther.* **2019**, *14*, 93–116. [CrossRef]

Mar. Drugs **2021**, 19, 556

3. Ahmed, S.; Ikram, S. Chitosan Based Scaffolds and Their Applications in Wound Healing. *Achiev. Life Sci.* **2016**, *10*, 27–37. [CrossRef]

- 4. Azad, A.K.; Sermsintham, N.; Chandrkrachang, S.; Stevens, W.F. Chitosan membrane as a wound-healing dressing: Characterization and clinical application. *J. Biomed. Mater. Res.* **2004**, *69*, 216–222. [CrossRef]
- 5. Lee, E.-J.; Shin, D.-S.; Kim, H.-E.; Kim, H.-W.; Koh, Y.-H.; Jang, J.-H. Membrane of hybrid chitosan–Silica xerogel for guided bone regeneration. *Biomaterials* **2009**, *30*, 743–750. [CrossRef]
- 6. Murali, V.P.; Fujiwara, T.; Gallop, C.; Wang, Y.; Wilson, J.A.; Atwill, M.T.; Kurakula, M.; Bumgardner, J.D. Modified electrospun chitosan membranes for controlled release of simvastatin. *Int. J. Pharm.* **2020**, *584*, 119438. [CrossRef]
- 7. Niemczyk, A.; Kmieciak, A.; El Fray, M.; Piegat, A. The influence of c18-fatty acids on chemical structure of chitosan derivatives and their thermal properties. *Prog. Chem. Appl. Chitin Deriv.* **2016**, *21*, 165–175. [CrossRef]
- 8. Efiana, N.A.; Mahmood, A.; Lam, H.T.; Zupančič, O.; Leonaviciute, G.; Bernkop-Schnürch, A. Improved mucoadhesive properties of self-nanoemulsifying drug delivery systems (SNEDDS) by introducing acyl chitosan. *Int. J. Pharm.* **2017**, *519*, 206–212. [CrossRef]
- 9. Costa, F.; Sousa, D.; Parreira, P.; Lamghari, M.; Gomes, P.; Martins, M.C.L. N-acetylcysteine-functionalized coating avoids bacterial adhesion and biofilm formation. *Sci. Rep.* **2017**, *7*, 1–13. [CrossRef]
- 10. Dang, Q.; Zhang, Q.; Liu, C.; Yan, J.; Chang, G.; Xin, Y.; Cheng, X.; Cao, Y.; Gao, H.; Liu, Y. Decanoic acid functionalized chitosan: Synthesis, characterization, and evaluation as potential wound dressing material. *Int. J. Biol. Macromol.* **2019**, 139, 1046–1053. [CrossRef]
- 11. Bonferoni, M.; Sandri, G.; Dellera, E.; Rossi, S.; Ferrari, F.; Mori, M.; Caramella, C. Ionic polymeric micelles based on chitosan and fatty acids and intended for wound healing. Comparison of linoleic and oleic acid. *Eur. J. Pharm. Biopharm.* **2013**, 87, 101–106. [CrossRef]
- 12. Zhang, Z.; Jin, F.; Wu, Z.; Jin, J.; Li, F.; Wang, Y.; Wang, Z.; Tang, S.; Wu, C.; Wang, Y. O-acylation of chitosan nanofibers by short-chain and long-chain fatty acids. *Carbohydr. Polym.* **2017**, 177, 203–209. [CrossRef]
- 13. Wu, C.; Su, H.; Karydis, A.; Anderson, K.M.; Ghadri, N.; Tang, S.; Wang, Y.-F.; Bumgardner, J.D. Mechanically stable surface-hydrophobilized chitosan nanofibrous barrier membranes for guided bone regeneration. *Biomed. Mater.* **2017**, *13*, 015004. [CrossRef]
- 14. Wu, C.; Su, H.; Tang, S.; Bumgardner, J.D. The stabilization of electrospun chitosan nanofibers by reversible acylation. *Cellulose* **2014**, *21*, 2549–2556. [CrossRef]
- 15. Ferreira, M.O.G.; Lima, I.S.; Ribeiro, A.B.; Lobo, A.O.; Rizzo, M.S.; Osajima, J.A.; Estevinho, L.M.; Silva-Filho, E.C. Biocompatible Gels of Chitosan–Buriti Oil for Potential Wound Healing Applications. *Materials* **2020**, *13*, 1977. [CrossRef]
- 16. Hasegawa, M.; Isogai, A.; Onabe, F.; Usuda, M. Dissolving states of cellulose and chitosan in trifluoroacetic acid. *J. Appl. Polym. Sci.* **1992**, 45, 1857–1863. [CrossRef]
- 17. Xu, J.; McCarthy, S.P.; Gross, R.A.; Kaplan, D.L. Chitosan Film Acylation and Effects on Biodegradability. *Macromolecules* **1996**, 29, 3436–3440. [CrossRef]
- 18. Le Tien, C.; Lacroix, M.; Ispas-Szabo, P.; Mateescu, M.-A. N-acylated chitosan: Hydrophobic matrices for controlled drug release. *J. Control. Release* **2003**, *93*, 1–13. [CrossRef]
- 19. Jaeger, K.E.; Steinbüchel, A.; Jendrossek, D. Substrate specificities of bacterial polyhydroxyalkanoate depolymerases and lipases: Bacterial lipases hydrolyze poly(omega-hydroxyalkanoates). *Appl. Environ. Microbiol.* **1995**, *61*, 3113–3118. [CrossRef]
- 20. Jendrossek, D. Microbial degradation of polyesters: A review on extracellular poly (hydroxyalkanoic acid) depolymerases. *Polym. Degrad. Stab.* **1998**, *59*, 317–325. [CrossRef]
- 21. Tay, F.R.; Pashley, D.H.; Williams, M.C.; Raina, R.; Loushine, R.J.; Weller, R.N.; Kimbrough, W.F.; King, N.M. Susceptibility of a Polycaprolactone-based Root Canal Filling Material to Degradation. I. Alkaline Hydrolysis. *J. Endod.* 2005, 31, 593–598. [CrossRef]
- 22. Redington, R.L.; Lin, K.C. Infrared spectra of trifluoroacetic acid and trifluoroacetic anhydride. *Spectroschim. Acta Part A Mol. Spectrosc.* **1971**, 27, 2445–2460. [CrossRef]
- 23. Standardization, I.O.F. Biological Evaluation of Medical Devices—Part 5: Tests for In Vitro Cytotoxicity. 2009. Available online: https://webstore.ansi.org/preview-pages/BSI/preview_30356171.pdf (accessed on 26 September 2021).
- 24. Harrison, Z.L.; Awais, R.; Harris, M.; Raji, B.; Hoffman, B.C.; Baker, D.L.; Jennings, J.A. 2-Heptylcyclopropane-1-Carboxylic Acid Disperses and Inhibits Bacterial Biofilms. *Front. Microbiol.* **2021**, *12*, 1298. [CrossRef] [PubMed]
- 25. Marques, C.N.H.; Davies, D.G.; Sauer, K. Control of Biofilms with the Fatty Acid Signaling Molecule cis-2-Decenoic Acid. *Pharmaceuticals* **2015**, *8*, 816–835. [CrossRef]
- 26. Leceta, I.; Guerrero, P.; de la Caba, K. Functional properties of chitosan-based films. *Carbohydr. Polym.* **2012**, 93, 339–346. [CrossRef]
- 27. Bumgardner, J.D.; Wiser, R.; Elder, S.H.; Jouett, R.; Yang, Y.; Ong, J.L. Contact angle, protein adsorption and osteoblast precursor cell attachment to chitosan coatings bonded to titanium. *J. Biomater. Sci. Polym. Ed.* **2003**, *14*, 1401–1409. [CrossRef]
- 28. Hong, P.Z.; Li, S.D.; Ou, C.Y.; Li, C.P.; Yang, L.; Zhang, C.H. Thermogravimetric analysis of chitosan. *J. Appl. Polym. Sci.* **2007**, *105*, 547–551. [CrossRef]
- 29. Wang, J.; Wang, H. Preparation of soluble p-aminobenzoyl chitosan ester by Schiff's base and antibacterial activity of the derivatives. *Int. J. Biol. Macromol.* **2011**, *48*, 523–529. [CrossRef]

Mar. Drugs **2021**, 19, 556

30. Feng, Y.; Xia, W. Preparation, characterization and antibacterial activity of water-soluble O-fumaryl-chitosan. *Carbohydr. Polym.* **2011**, *83*, 1169–1173. [CrossRef]

- 31. O'Toole, G.A.; Kolter, R. Flagellar and twitching motility are necessary for pseudomonas aeruginosa biofilm development. *Mol. Microbiol.* **1998**, *30*, 295–304. [CrossRef]
- 32. Klausen, M.; Heydorn, A.; Ragas, P.; Lambertsen, L.; Aaes-Jørgensen, A.; Molin, S.; Tolker-Nielsen, T. Biofilm formation by Pseudomonas aeruginosa wild type, flagella and type IV pili mutants. *Mol. Microbiol.* **2003**, *48*, 1511–1524. [CrossRef]
- 33. Qi, L.; Christopher, G.F. Role of Flagella, Type IV Pili, Biosurfactants, and Extracellular Polymeric Substance Polysaccharides on the Formation of Pellicles by Pseudomonas aeruginosa. *Langmuir* **2019**, *35*, 5294–5304. [CrossRef] [PubMed]
- 34. Moormeier, D.E.; Bayles, K.W. Staphylococcus aureus biofilm: A complex developmental organism. *Mol. Microbiol.* **2017**, *104*, 365–376. [CrossRef] [PubMed]
- 35. Reifsteck, F.; Wee, S.; Wilkinson, B.J. Hydrophobicity—Hydrophilicity of staphylococci. *J. Med. Microbiol.* **1987**, 24, 65–73. [CrossRef]
- 36. Bruinsma, G.; van der Mei, H.; Busscher, H. Bacterial adhesion to surface hydrophilic and hydrophobic contact lenses. *Biomaterials* **2001**, 22, 3217–3224. [CrossRef]
- 37. Chen, W.; Cheng, C.-A.; Lee, B.-Y.; Clemens, D.L.; Huang, W.-Y.; Horwitz, M.A.; Zink, J.I. Facile Strategy Enabling Both High Loading and High Release Amounts of the Water-Insoluble Drug Clofazimine Using Mesoporous Silica Nanoparticles. *ACS Appl. Mater. Interfaces* **2018**, *10*, 31870–31881. [CrossRef]
- 38. Taaca, K.L.M.; Vasquez, M.R., Jr. Hemocompatibility and cytocompatibility of pristine and plasma-treated silver-zeolite-chitosan composites. *Appl. Surf. Sci.* **2018**, 432, 324–331. [CrossRef]
- 39. Sathiyaseelan, A.; Saravanakumar, K.; Mariadoss, A.; Wang, M.-H. Antimicrobial and Wound Healing Properties of FeO Fabricated Chitosan/PVA Nanocomposite Sponge. *Antibiotics* **2021**, *10*, 524. [CrossRef]
- 40. Mariadoss, A.V.A.; Vinayagam, R.; Senthilkumar, V.; Paulpandi, M.; Murugan, K.; Xu, B.; Gothandam, K.M.; Kotakadi, V.S.; David, E. Phloretin loaded chitosan nanoparticles augments the ph-dependent mitochondrial-mediated intrinsic apoptosis in human oral cancer cells. *Int. J. Biol. Macromol.* 2019, 130, 997–1008. [CrossRef] [PubMed]
- 41. Smith, K.J.; Moshref, A.R.; Jennings, J.A.; Courtney, H.S.; Haggard, W.O. Chitosan Sponges for Local Synergistic Infection Therapy: A Pilot Study. *Clin. Orthop. Relat. Res.* **2013**, 471, 3158–3164. [CrossRef] [PubMed]
- 42. Parker, A.C.; Jennings, J.A.; Bumgardner, J.D.; Courtney, H.S.; Lindner, E.; Haggard, W.O.; Lindner, E. Preliminary investigation of crosslinked chitosan sponges for tailorable drug delivery and infection control. *J. Biomed. Mater. Res. Part B Appl. Biomater.* **2012**, *101*, 110–123. [CrossRef] [PubMed]
- 43. Harrison, Z.L.; Bumgardner, J.D.; Fujiwara, T.; Baker, D.L.; Jennings, J.A. In vitro evaluation of loaded chitosan membranes for pain relief and infection prevention. *J. Biomed. Mater. Res. Part B Appl. Biomater.* **2021**, *11*, 1735–1743. [CrossRef]
- 44. Sathiyaseelan, A.; Saravanakumar, K.; Mariadoss, A.V.A.; Wang, M.H. pH-controlled nucleolin targeted release of dual drug from chitosan-gold based aptamer functionalized nano drug delivery system for improved glioblastoma treatment. *Carbohydr. Polym.* **2021**, 262, 117907. [CrossRef] [PubMed]
- 45. Kasaai, M.R. Calculation of Mark–Houwink–Sakurada (MHS) equation viscometric constants for chitosan in any solvent–temperature system using experimental reported viscometric constants data. *Carbohydr. Polym.* **2007**, *68*, 477–488. [CrossRef]
- 46. Kasaai, M.R.; Arul, J. Intrinsic viscosity-molecular weight relationship for chitosan. *J. Polym. Sci. Part B Polym. Phys.* **2000**, *38*, 2591–2598. [CrossRef]
- 47. Namazi, H.; Dadkhah, A. Convenient method for preparation of hydrophobically modified starch nanocrystals with using fatty acids. *Carbohydr. Polym.* **2010**, *79*, 731–737. [CrossRef]